Proceedings of ASME Turbo Expo 2011
GT2011
June 6-10, 2011, Vancouver, British Columbia, Canada

GT2011-46189

HEAT TRANSFER ENHANCEMENT IN TIP-TURN REGION OF TWO-PASS CHANNEL WITH A 180-DEGREE TURN

Pavin Ganmol
University of Pittsburgh
Pittsburgh, PA, USA

Minking K. Chyu
University of Pittsburgh
Pittsburgh, PA, USA

Mary Anne Alvin
National Energy Technology Laboratory
Pittsburgh, PA, USA

ABSTRACT

The design geometry and transport phenomena associated with the tip internal cooling can be very complex and has been little studied. Internal cooling channel near a tip region typically inherits a sharp, 180-degree, turn and little or no enhancement installation exists. To explore potential design for enhancement cooling, a series of experiments are performed to investigate the heat transfer enhancement by placing different pin-fins configurations in the tip-turn region of a two-pass channel with a 180-degree sharp turn. Transient liquid crystal technique is applied to acquire detailed local heat transfer data both on the channel surface and pin elements, for Reynolds number between 13,000 and 28,000. Present results suggest that the pin-fins can enhance heat transfer up to 2.3 fold in the tip-turn region and up to 1.3 fold for the entire channel. The presence of the pin-fins also changes the flow pattern in the post turn region which is resulting in more evenly distributed heat transfer downstream of the turn.

INTRODUCTION

Gas turbines are subjected to continuous demand for improvements in efficiency and performance. To increase thermal efficiency, gas turbines need to be operated at the highest possible inlet temperature. Combustion gas temperature upstream of the turbine stage is in the order of 2000 °C, which is well above the melting temperature of component metals, even for the most advanced superalloys. One of the most challenging tasks for turbine designers is to develop the cooling system that can maintain the turbine components temperature under their metallurgical limits. For internal cooling, coolant passages inside the bulk of an airfoil are arranged in serpentine configurations with 180-degree sharp turns. Earlier studies [1] have suggested that, while an 180-degree turn can cause non-uniform cooling in the turning region, the sharp turn, in fact, can render a higher heat transfer in the passage overall. However, the level of such turn-induced heat transfer enhancement varies with the actual turn geometry [2]. In addition, passage aspect ratio also has significant effects on the heat transfer and flow characteristics in the channel [3]. Cooling channels with a high aspect ratio are generally of higher friction factor and pressure loss than low aspect ratio channels. However, they can perform better and consume less coolant when strategically placed in a turbine airfoil.

Surface features such as pin-fins are usually incorporated on the surfaces of turbine internal cooling passages to promote turbulent transport, therefore enhancing convective heat transfer. The pins in the flow field create the wake downstream and generate horseshoe vortices at the base of the pins. In additional to turbulence promotion, pin-fins could add more heat transfer area in a cooling channel, provided that the pin length-to-diameter ratio, L/D, is sufficiently large. However, this effect is rather limited for turbine applications, as pin-fins have been used primarily for cooling of the airfoil's trailing edge where the short channel height dictates the usage of pin-fins with L/D ~ 1. Armstrong and Winstanley [4] compiled heat transfer and pressure loss data for short pin-fins configured in staggered arrays prior to mid 1980's. These data suggest short aspect ratio pin-fins renders lower heat transfer than their longer aspect ratio counterparts, due mainly to impeded vortex generation by the narrowly spaced endwalls. Since then, various aspects of transport phenomena associated with short pin-fins have been actively studied and reported in the open literature [5-9]. Meanwhile, advancement in the airfoil casting technology has recently permitted pin-fins to be used for cooling of the airfoils main body [10, 11]. Cooling of the tip region of a turbine airfoil is known to be difficult, due mainly to its exposure to hot tip leakage flow and limited cooling area. Current technology for tip cooling relies mostly on external cooling by injecting film coolant in the tip vicinity. Since

external cooling is known to be aerodynamically inefficient, the state-of-the-art approach calls for utilization of internal cooling.

The purpose of this study is to explore the heat transfer characteristics of the cooling design in the tip-turn region of a 2-pass channel with a 180-degree sharp turn. Different pin-fin configurations are arranged in the turning region to manage the gas flow path and to promote heat transfer on all of the channel's endwalls. Currently, reported results or data similar to our study, which emphasizes in promoting heat transfer in the turning region, are not found in the open literatures. One of the objectives of this study is to establish an experimental model that permits a simultaneous measurement of heat transfer from all participating surfaces, including both pin-fins and all endwall surfaces. To acquire the local heat transfer coefficient from these surfaces, the present measurement employs a hybrid measurement technique based on transient liquid crystal imaging. The hybrid technique employs the transient conduction model in a semi-infinite solid for resolving the heat transfer coefficient on the surfaces. The heat transfer coefficient over a pin element can be resolved by the lumped capacitance method with a reasonable assumption of low Biot number. The Reynolds numbers based on the mean gas flow velocity and hydraulic diameter of the channel are 13,000, 20,000 and 28,000.

NOMENCLATURE

A area (m^2)
f_0 friction factor of the smooth channel with no turn
f_{ave} friction factor of the channel
C_p volumetric heat capacity (kJ/kg-K)
D channel width/depth (m)
D_h hydraulic diameter (m)
d pin diameter (m)
h heat transfer coefficient (W/m^2-K)
k thermal conductivity (W/m-K)
m mass (kg)
Nu Nusselt number, hD_h/k
q heat flux (W/m^2)
Re_{Dh} Reynolds number, UD_h/υ
t time (s)
T temperature (K)
T_i initial temperature (K)
T_r the flow reference temperature (K)
T_w wall temperature (K)
U flow velocity (m/s)
z coordinate direction into the substrate (m)

Greek Symbols

α thermal diffusivity, $k/(\rho C_p)$ (m^2/s)
ρ mass density (kg/m^3)
Δp pressure drop across the channel (Pa)

THEORY

Transient liquid crystal technique is a useful and effective technique which has become one of the standard techniques for determining heat transfer coefficient, h, for several years. By assuming that the transient conduction in the semi-infinite solid is one-dimensional, as shown in Figure 1, the local heat transfer coefficient can be determined. The temperature field in the solid, T, is governed by the one-dimensional transient heat conduction equation and boundary and initial conditions.

$$k\frac{\partial^2 T}{\partial z^2} = \rho C_p \frac{\partial T}{\partial t} \tag{1}$$

$$-k\left.\frac{\partial T}{\partial z}\right|_{z=0} = h(T_w - T_r) \tag{2}$$

$$T\big|_{z=\infty} = T_i \tag{3}$$

$$T\big|_{t=0} = T_i \tag{4}$$

where T_i is initial temperature of the channel wall and T_w is the local surface temperature of the channel wall. T_r is the flow reference temperature. From the equation (1)-(4), wall temperature T_w can be expressed as

$$\frac{T_w - T_i}{T_r - T_i} = 1 - \exp\left[\frac{h^2\alpha t}{k^2}\right] erfc\left[\frac{h\sqrt{\alpha t}}{k}\right] \tag{5}$$

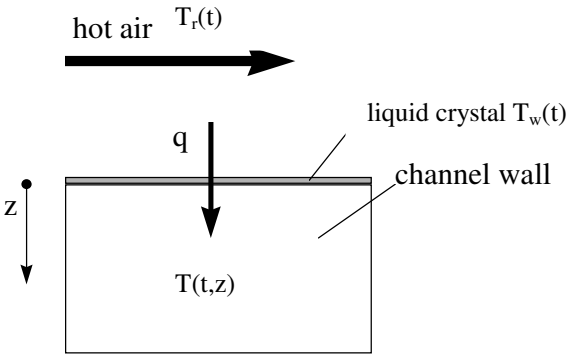

Figure 1. One-Dimensional Heat Transfer over Solid Surface

In classical heat convection problems, the reference temperature T_r is readily available, i.e. equal to the temperature of the mainstream or bulk flow. Liquid crystal imaging can provide a relation between T_w and t over the entire capturing domain and the local heat transfer coefficient, h, can be solved from the above equation.

While the above approach is generally valid for the channel wall, it is not applicable for the turbulator elements that are placed on the channel wall since they are of three-dimensional geometry with heat conduction occurring in three dimensions. To obtain the heat transfer coefficient of a turbulator, lumped capacitance method has been used under the assumption that the element has uniform temperature (small Biot number) at all times, due to high thermal conductivity and its small size. The

governing equation for lumped heat capacity model and initial condition are

$$hA(T - T_r) = -mC_p \frac{dT}{dt} \tag{6}$$

$$T\big|_{t=0} = T_i \tag{7}$$

From the above equation, an analytic solution can be obtained as

$$\frac{T - T_i}{T_r - T_i} = 1 - \exp\left[-\frac{hAt}{mC_p}\right] \tag{8}$$

EXPERIMENTAL SETUP

In this study, a series of experiments are performed to investigate the heat transfer and pressure characteristics in turning region of a two-pass channel with various pin-fin configurations. The transient liquid crystal technique is applied to acquire detailed local heat transfer data both on the channel surface and pin elements, for Reynolds numbers between 13,000 and 28,000.

Figure 2 shows the 2-pass channel without pin-fin (baseline configuration). The test section is fabricated using a 0.5-inch thick Plexiglas plates. The channel dimension is 381.0 mm x 57.2 mm x 12.7 mm (15"x2.25"x0.5") (width x length x height). Figure 3 shows seven pin-fin channel configurations. The pin-fins are placed in the channel to enhance heat transfer in the turning region. In an attempt to spread the flow evenly and to direct the flow to the corners of the channel which usually have low heat transfer coefficient, a number of pin-fin configurations are examined. The pin diameter, d, is 6.4 mm (0.25"). The surfaces of the channel and the pins are treated with thermochromic liquid crystal which changes color when exposed to heat. Preliminary tests are performed for all seven configurations. From the preliminary results, the top three performers, i.e. the pin-fin configurations 5, 6 and 7, were chosen along with the baseline to be fully investigated.

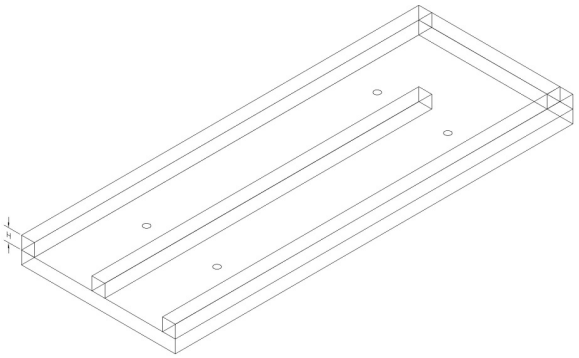

Figure 2. Two-Pass Channel with 180-Degree Sharp Turn

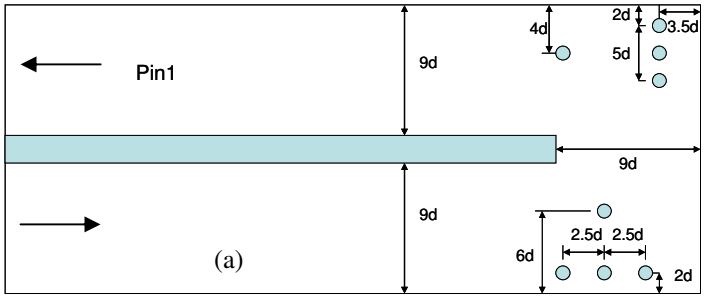

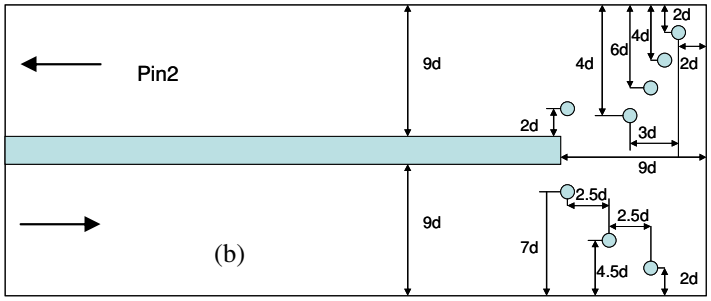

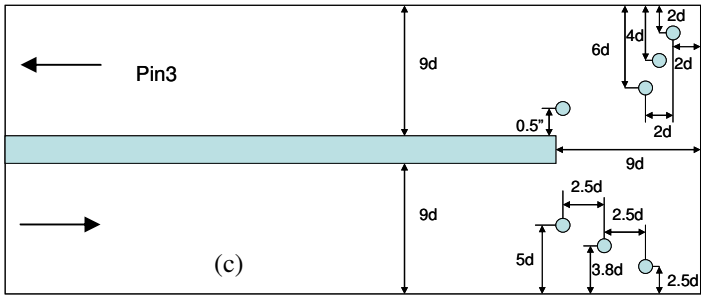

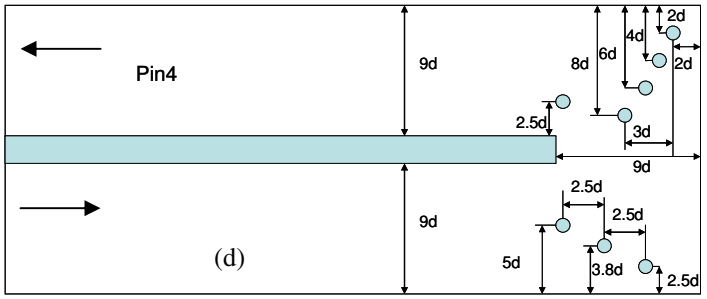

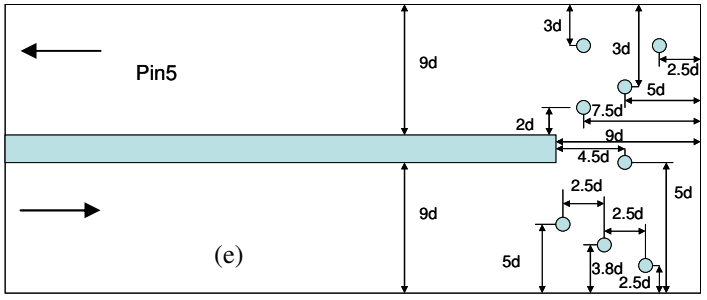

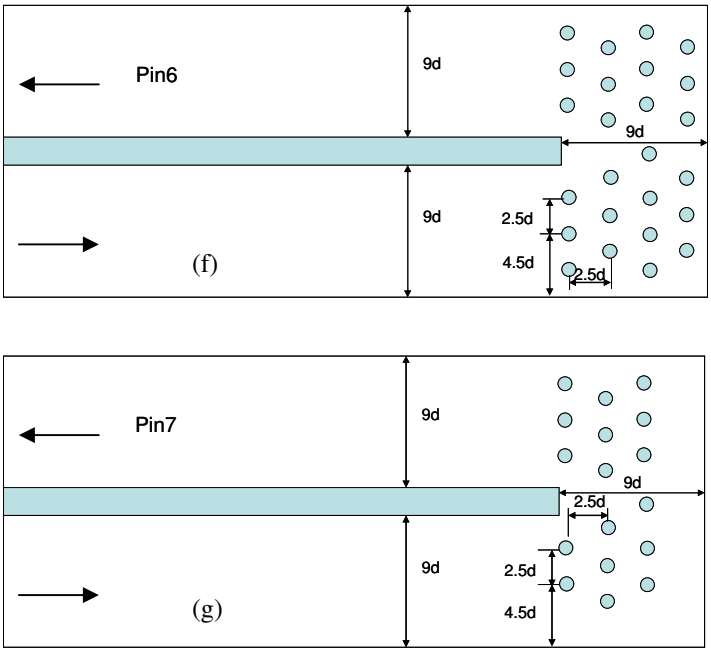

Figure 3. Two-Pass Channel with Pin-Fin Configurations

The experimental set up is shown in Figure 4. An air compressor provides the main flow. The flow rate is measured by standard ASME orifice and can be adjusted by a ball valve before the orifice. After passing through the orifice, the flow passes through an inline heater controlled by a variable voltage controller. The temperature of flow is controlled accurately to a desired level of 80°C. During the warm-up period, the flow is diverted away from the test section. When the desired steady temperature is reached, the valve is turned to direct the flow to the test section. The digital camcorder records the color changing video images of the surface while the data acquisition equipment is registering the temperatures of the mainstream flow. After the digital video file and the temperature data history are combined and analyzed with liquid crystal imaging analyzer (LCIA) software, the local heat transfer coefficient is obtained.

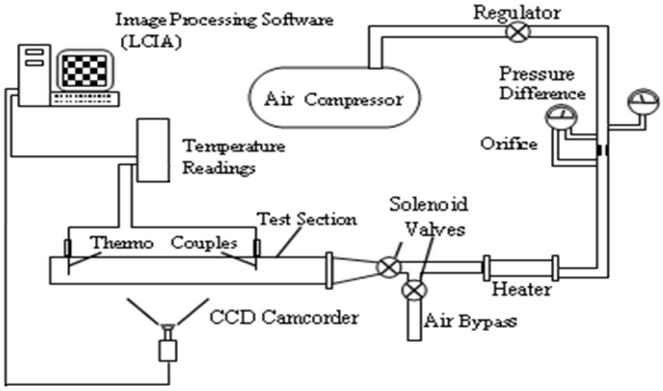

Figure 4. Experiment Setup Diagram

RESULTS AND DISCUSSION

The heat transfer results are presented by a dimensionless heat transfer coefficient, i.e. Nusselt number, Nu, which is defined as

$$Nu = \frac{hD_h}{k} \tag{9}$$

where h is a local or regional averaged heat transfer coefficient and D_h is the hydraulic diameter. The previous term can be normalized by the fully developed value of the turbulent flow in the smooth duct without turn, Nu_0, which is

$$Nu_0 = 0.023\,\mathrm{Re}^{0.8}\,\mathrm{Pr}^{0.4} \tag{10}$$

The uncertainty analysis on the Nusselt number, Nu, with a 95% confidence level is based on the method of Kline and McClintock [12]. The present liquid crystal method depends strongly on the temperature measurement which has uncertainties of about ±0.2°C. In addition, the uncertainty of Nu is also affected by errors in color calibration of the liquid crystal and also error in measuring flow rate. All the combined errors lead to the overall 8% uncertainty in Nu.

The Local Heat Transfer Coefficient Distribution

Figure 5-8 show the localized heat transfer coefficient distributions in a two-pass channel. The left-hand sides of the figures show the entire of the first and second pass endwalls while the right-hand sides show the detail heat transfer of the turning region.

Figure 5 shows the localized heat transfer coefficient distributions in a two-pass channel without pin-fins. The figure shows that the average heat transfer in the second pass of the channel is much higher as a result of the sharp turn effect. The sharp turn induces strong secondary flow and turbulence in the second pass; thus the heat transfer in the second pass is approximately 37% higher than that of the first pass over the range of 13,000-28,000 Reynolds number. In the tip-turn region, the second side endwall also exhibits significantly higher heat transfer than the first side endwall. The results show a similar heat transfer distribution trend as the study by Wang and Chyu [13]. The other significant feature observed in Figure 5 is that the heat transfer coefficient is rather low at the turn corners and in the vicinity of the tip of the partition wall. This phenomenon occurs mainly due to the nature of flow and geometry (sharp corner) of the test section that creates a recirculation zone at those particular regions.

Figure 6 shows the localized heat transfer coefficient distributions in a two-pass channel with Pin#5 configuration in the tip-turn region. With a small number of pins in each pass before and after the turn, the flow characteristic and heat transfer distribution are altered subtly. The transport phenomena in the second pass are still highly influenced by the180-degree sharp turn. While the pin-fins can enhance heat transfer in the turning region up to 1.3 fold, the overall average

heat transfer of the entire channel has no significant gain as shown in Tables 1 and 2.

Figure 7 shows the localized heat transfer coefficient distributions in a two-pass channel with Pin#6 configuration in the tip-turn region. The figure remarkably reveals that the staggered pin-fin arrays significantly change the flow and heat transfer characteristic in the turning region. The pin-fin arrays create more turbulent flow, spreading the flow in the turning region, thus resulting in more even heat transfer distribution with reduction of the recirculation zones. While the Pin#6 configuration yields up to 1.3 fold heat transfer enhancement for the entire channel, the heat transfer enhancement in the turning region is up to 2 fold.

Pin#7 configuration is the resulting effort to reduce pressure loss for the Pin#6 configuration. The heat transfer results of the Pin#7 configuration are shown in Figure 8. The figure reveals that the heat transfer distribution trend is similar to that of the Pin#6 configuration. The tip and second side endwalls heat transfer is higher than that of the Pin#6 configuration, but the other endwall and overall heat transfer is lower. Compared to the baseline, Pin#7 configuration can enhance heat transfer up to 1.2 fold for the entire channel and up to 1.6 fold in the turning region. Table 1 shows the average heat transfer coefficient in the entire channel for all the configurations presented in this study. While insignificant heat transfer enhancement is shown for Pin#5 configuration, the Pin#6 and Pin#7 configurations heat transfer enhancement is substantial.

Table 2 and Figure 5 show that with the small number of pin-fins placed in the turning region, heat transfer can be enhanced subtly on all of the endwall surfaces with the exception that heat transfer becomes lower on the second side endwall relative to the baseline configuration. When large numbers of pin-fins are placed in the turning region, heat transfer is enhanced significantly on all of the endwalls except the second side endwall.

Heat Transfer Coefficient (W/m^2-K)								
Re_{Dh}	Endwall	Baseline	Pin#5	/Baseline	Pin#6	/Baseline	Pin#7	/Baseline
13,000	1st pass	67	70	1.04	81	1.22	74	1.10
	2nd pass	91	89	0.98	110	1.21	100	1.10
20,000	1st pass	89	91	1.03	114	1.29	99	1.11
	2nd pass	123	119	0.97	151	1.23	132	1.07
28,000	1st pass	118	124	1.05	162	1.37	138	1.17
	2nd pass	163	162	0.99	204	1.26	189	1.16

Table 1: Average Heat transfer Coefficient of the Channel

Heat Transfer Coefficient (W/m^2-K)								
Re_{Dh}	Endwall	Baseline	Pin#5	/Baseline	Pin#6	/Baseline	Pin#7	/Baseline
13,000	1st pass	75	102	1.36	139	1.86	115	1.54
	2nd pass	104	129	1.24	184	1.77	164	1.57
	1st side	23	34	1.44	39	1.67	34	1.48
	2nd side	97	90	0.93	75	0.77	95	0.98
	Tip	61	68	1.11	77	1.25	77	1.26
20,000	1st pass	97	130	1.34	189	1.94	152	1.56
	2nd pass	134	169	1.26	254	1.89	217	1.61
	1st side	41	47	1.17	56	1.38	52	1.28
	2nd side	160	115	0.72	100	0.62	128	0.80
	Tip	90	95	1.06	103	1.15	104	1.16
28,000	1st pass	129	174	1.35	306	2.37	220	1.71
	2nd pass	174	231	1.33	384	2.21	330	1.90
	1st side	51	62	1.22	73	1.42	68	1.33
	2nd side	196	153	0.78	134	0.68	175	0.89
	Tip	115	121	1.05	137	1.19	139	1.21

Table 2: Average Heat transfer Coefficient in the Turning Region

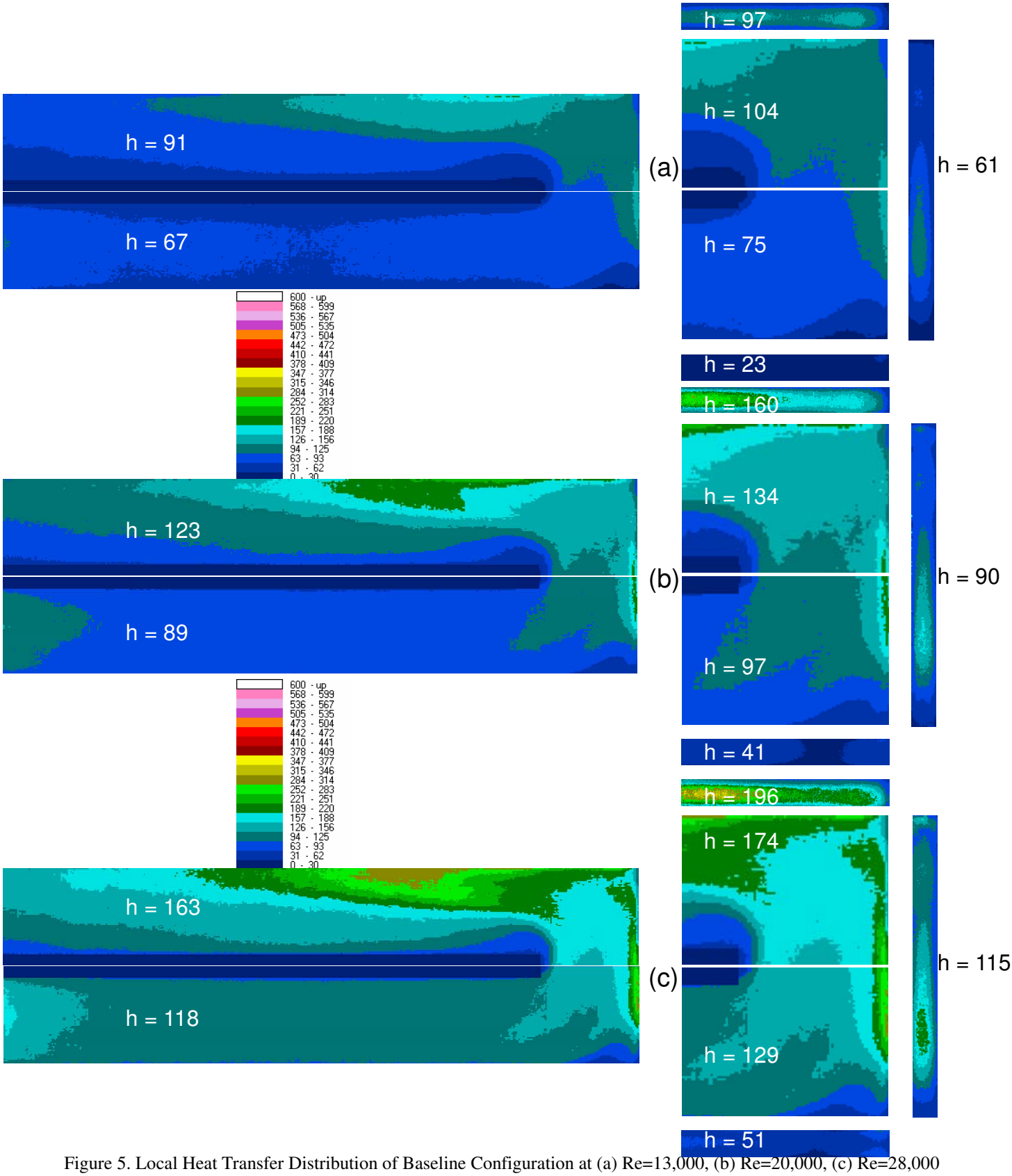

Figure 5. Local Heat Transfer Distribution of Baseline Configuration at (a) Re=13,000, (b) Re=20,000, (c) Re=28,000

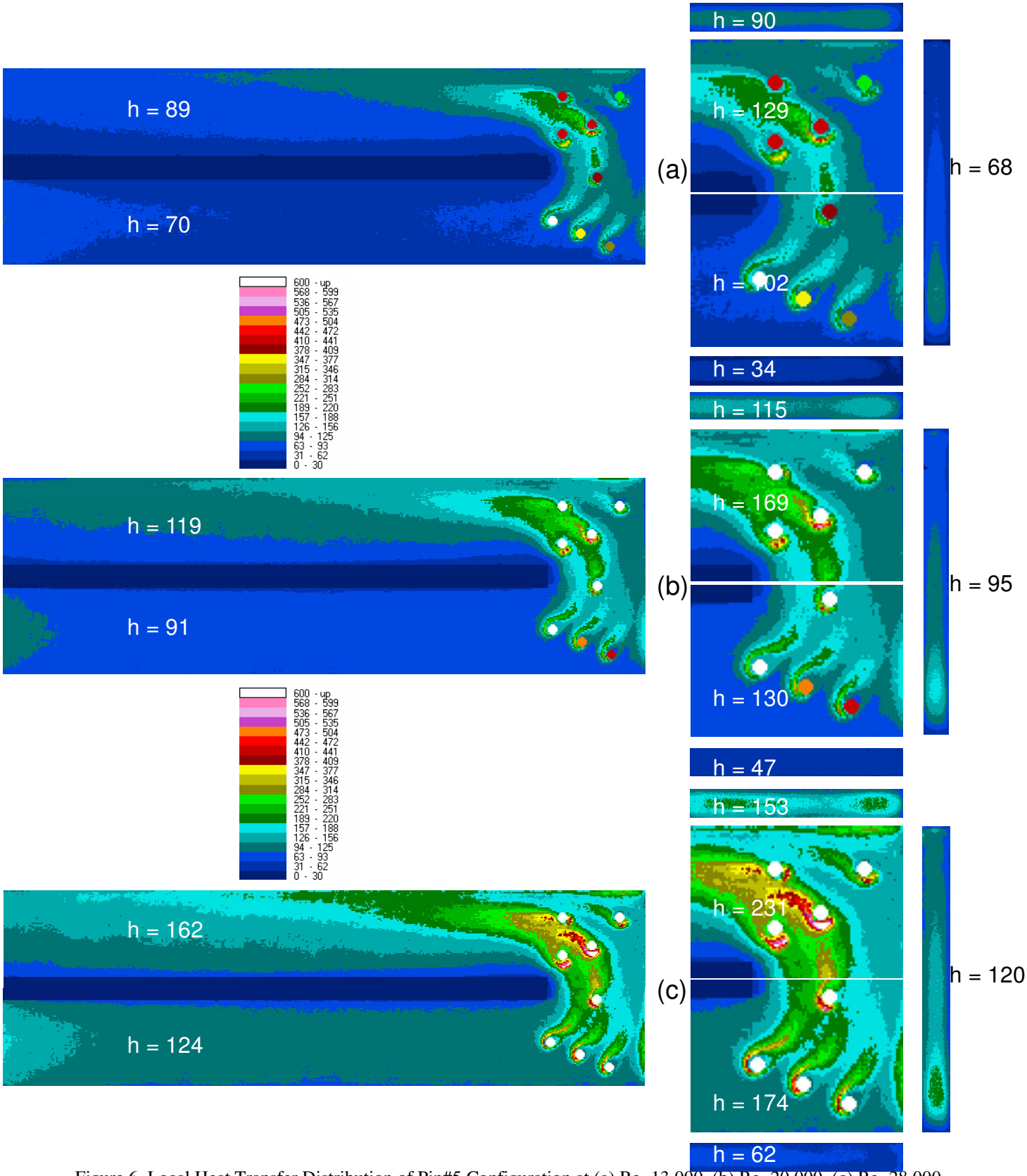

Figure 6. Local Heat Transfer Distribution of Pin#5 Configuration at (a) Re=13,000, (b) Re=20,000, (c) Re=28,000

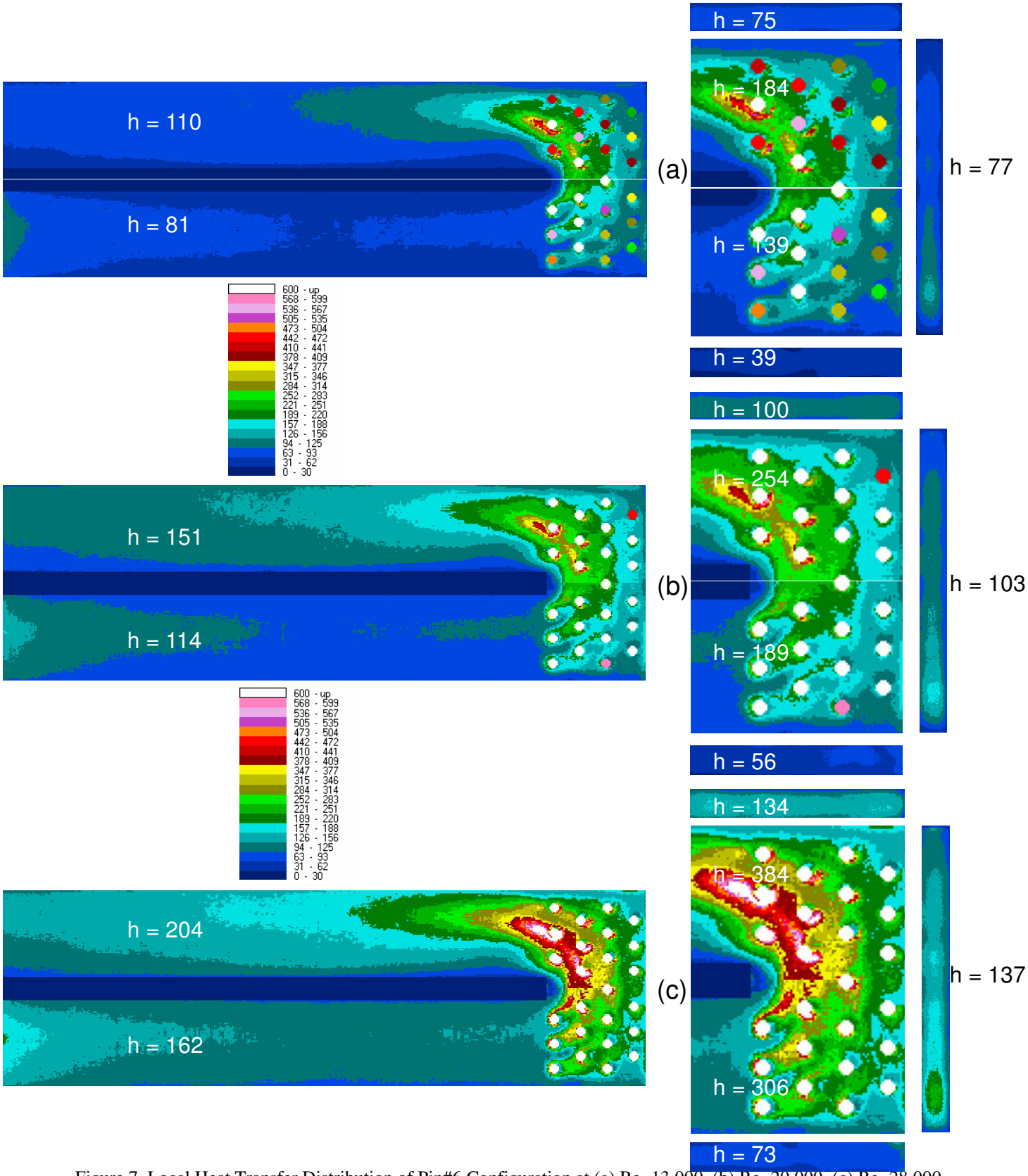

Figure 7. Local Heat Transfer Distribution of Pin#6 Configuration at (a) Re=13,000, (b) Re=20,000, (c) Re=28,000

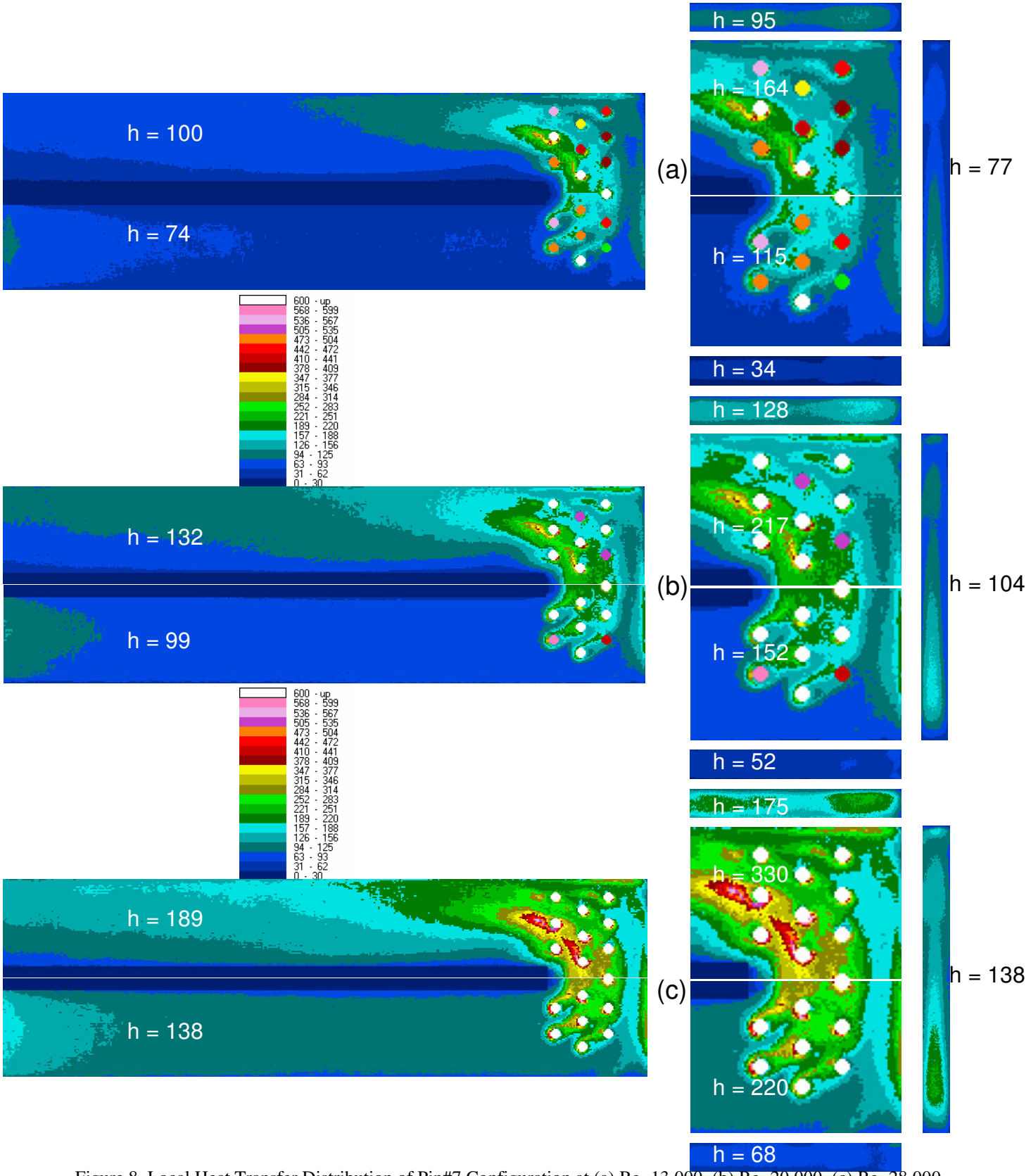

Figure 8. Local Heat Transfer Distribution of Pin#7 Configuration at (a) Re=13,000, (b) Re=20,000, (c) Re=28,000

The overall average heat transfer relation with the Reynolds number is shown in Figure 9. The experimental results show that the Pin#6 configuration, the staggered pin-fin arrays, achieves the highest heat transfer rate compared to all other configurations. Pin#7 configuration heat transfer rate falls between those of the baseline and Pin#6 while the Pin#5 configuration heat transfer is similar to that of the baseline. The overall results suggest that the density of pin-fins highly affects transport phenomena and heat transfer enhancement in the turning region.

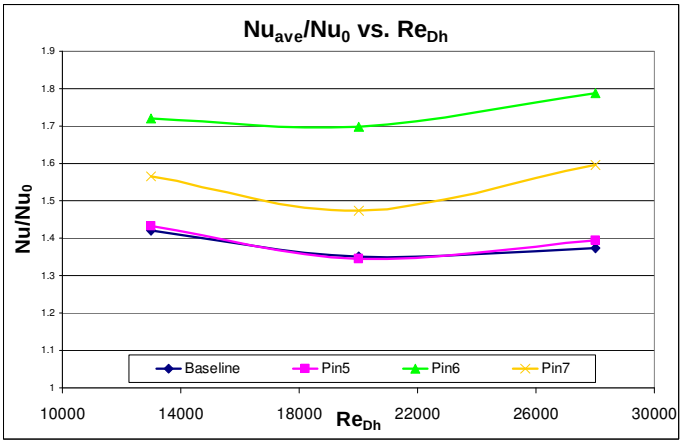

Figure 9. Comparison of Nu_{ave}/Nu_0 vs. Re_{Dh} with different channel configurations

Pressure Loss Coefficient

Heat transfer enhancement is always achieved at the expense of pressure loss. When pressure loss increases, more pumping power to maintain cooling flow is required which means that the overall efficiency of the gas turbine engine is decreased. Figure 10 shows pressure loss characteristics for the variation configurations, expressed as f_{ave}/f_0, where f_{ave} is the dimensionless friction factor

$$f_{ave} = \frac{\Delta p}{(\frac{L}{D_h})(\frac{\rho U^2}{2})} \qquad (11)$$

and the friction factor of the smooth channel with no turn, f_0, can be described as

$$f_0 = 0.316\,\mathrm{Re}^{-0.25} \qquad \mathrm{Re} \le 2 \times 10^4 \qquad (12)$$

$$f_0 = 0.184\,\mathrm{Re}^{-0.20} \qquad \mathrm{Re} \ge 2 \times 10^4 \qquad (13)$$

Figure 10 suggests that generally, the pressure loss of the Pin#6 configuration is the highest and can be up to 2.1 times of the baseline. Depending on the number of the pin-fins, the pressure loss penalty can be large.

Performance Factor

To compare the cooling performance of different channels, one must have a reference definition. According to the analysis by Gee and Webb [14], the definition of overall cooling performance factor can be expressed as

$$f_{PF} = \frac{f_N}{f_F^{1/3}} = \frac{Nu_{ave}/Nu_0}{(f_{ave}/f_0)^{1/3}} \qquad (14)$$

Figure 11 represents the overall cooling performance factors versus Reynolds number for the different channel configurations. All the pin configurations have higher cooling performance factor than that of the baseline. The Pin#6 configuration yields the highest cooling performance factor, followed by the Pin#7 and Pin#5 configurations.

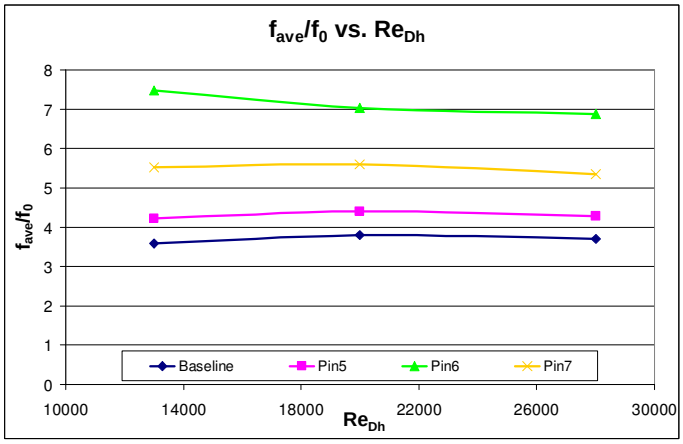

Figure 10. Comparison of f_{ave}/f_0 vs. Re_{Dh} with different channel configurations

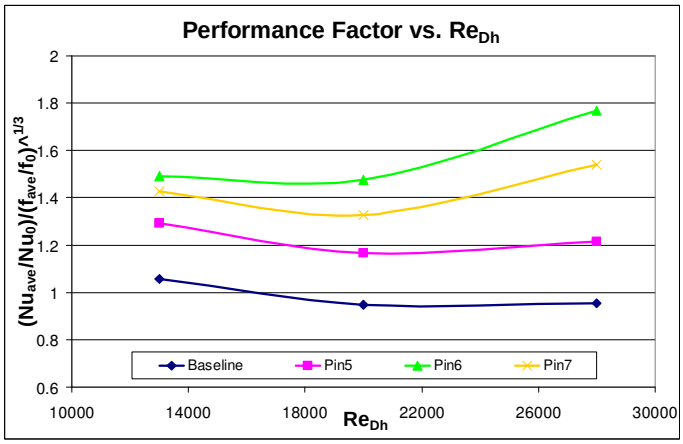

Figure 11. Overall cooling performance factor vs. Re_{Dh} with different channel configurations

CONCLUSIONS

The experimental study was performed to investigate heat transfer enhancement of pin-fins in the turning region of 2-pass channel with a 180-degree turn. Detailed heat transfer distribution was obtained by using a transient liquid crystal technique.

Current results suggest that the Pin#6 configuration, staggered pin-fin arrays in the turning region, has the highest heat transfer enhancement, and can enhance the heat transfer rate up to 2 fold in the turning region and up to 1.3 fold for the entire channel, relative to the fully-developed baseline smooth channel counterpart.

The presence of pin-fins in the turning region highly affects the flow and heat transfer distribution. With a small number of pins in each pass before and after the turn, the overall flow characteristic and heat transfer distribution are subtly changed but the heat transfer enhancement in the turning region can be significant. With a large number of pins placed in the turning region, i.e. Pin#6 and Pin#7 configurations, heat transfer and flow characteristics can be significantly changed, both in the turning and in the post turn regions.

It is interesting to note that all the pin-fin configurations can enhance heat transfer on all of endwall surfaces with the exception of the second side endwall. This result is due to pin-fin interference with the sharp turn effect in the post-turn region.

The heat transfer enhancement of the Pin#6 configuration is the highest among all the configurations but the pressure lost is also the highest. When pressure loss is considered, the Pin#6 configuration still demonstrates the highest cooling performance factor. The Pin#6 configuration is an optimal configuration in terms of both heat transfer enhancement and cooling performance criteria.

REFERENCES

[1] Metzger, D. E., and Sahm, M. K., 1986, "Heat Transfer Around Sharp 180-Deg Turn in Smooth Rectangular Channels," Journal of Heat Transfer, Vol. 108, No. 3, pp. 500-506.

[2] Wang, T., and Chyu, M. K., 1994, "Heat Convection in a 180-Deg Turning Duct with Different Turn Configurations," Journal of Thermophysics and Heat Transfer, Vol. 8, No. 3, pp. 595-601.

[3] Fan, C. S., and Metzger, D. E., 1987, "Effects of Channel Aspect ratio on Heat Transfer in Rectangular Passage Sharp 180-Deg turns," ASME Paper 87-GT-113

[4] Armstrong, J., and Winstanley, D., 1988, "A Review of Staggered Array Pin Fin Heat Transfer for Turbine Cooling Applications," ASME Journal of Turbomachinery, Vol. 110, pp. 94-103.

[5] Chyu, M. K., and Goldstein, R. J., 1991, "Influence of an Array of Wall-Mounted Cylinders on the Mass Transfer from a Flat Surface," International Journal of Heat and Mass Transfer, Vol. 34, No. 9, pp. 2175-2186.

[6] Chyu, M. K., Hsing, Y. C., Shih, T. I. P., and Natarajan, V., 1999, "Heat Transfer Contributions of Pins and Endwall in Pin-Fin Arrays: Effects of Thermal Boundary Condition Modeling," ASME Journal of Turbomachinery, Vol. 121, Vol. 2, pp. 257-263.

[7] Ames, F. E., and Dvorak, L. A., 2006, "Turbulent Transport in Pin Fin Arrays: Experimental Data and Predictions," Journal of Turbomachinery, Vol. 128, No.1, pp. 71-81

[8] Chyu, M. K., 1990, "Heat Transfer and Pressure Drop for Short Pin-Fin Arrays with Pin-Endwall Fillet," ASME Journal of Heat Transfer, Vol. 112, pp. 926-932.

[9] Goldstein, R. J., Jabbari, M. Y., and Chen, S. B., 1994, "Convective Mass Transfer and Pressure Loss Characteristics of Staggered Short Pin-Fin Arrays," International Journal of Heat and Mass Transfer, Vol. 37, Suppl. 1, pp. 149-160.

[10] European Patent Specification, EP 1 617 043 B1.

[11] Ganmol, P., Chyu, M. K., Chi, X., Shih, T. I-P., Alvin, M. A., 2010, "Effects of 90-Degree Jet Inlet on Heat Transfer from Staggered Pin Fin Arrays," ASME-ATI-UIT 2010 Conference on Thermal and Environmental Issues in Energy Systems, Sorrento, Italy.

[12] Kline, S. J., and McClintock, F. A., 1953, "Describing Uncertainties in Single-Sample Experiment," Mechanical Engineering, 75, pp. 3-8.

[13] Wang, T., and Chyu, M. K., 1994, "Heat Convection in a 180-Deg Turning Duct with Different Turn Configurations," Journal of Thermophysics and Heat Transfer, Vol. 8, No. 3., pp. 595-601.

[14] Gee, D. L., and Webb, R. L., 1980, "Forced convection Heat Transfer in Helically Rib-Roughened Tubes," International Journal of Heat and Mass Transfer, Vol. 23, pp. 1127-1136.